Radiología 65 (2023) S109–S119

RADIOLOGÍA

www.elsevier.es/rx

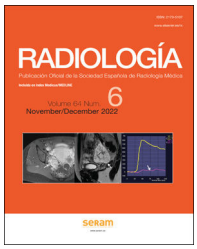

Spectral CT in Emergency

Helena Cigarrán Sexto*, **Juan Calvo Blanco**, **Gemma Fernández Suárez**

Hospital Universitario Central de Asturias, Oviedo, Asturias, Spain

Received 29 June 2022; accepted 9 November 2022

KEYWORDS
X-rays;
Computed tomography;
Emergency;
Dual energy

Abstract Spectral CT technology is based on the acquisition of CT images with X-ray at 2 different energy levels which makes possible to distinguish between materials with different atomic numbers using their energy-dependent attenuation, even if those materials have similar density at conventional CT.

This kind of technology has gained wide application due to the innumerable uses of their post-processing techniques, including virtual non-contrast images, iodine maps, virtual monochromatic images or mixed images without increasing radiation dose.

There are several applications of spectral CT in Emergency Radiology that help in the detection, diagnosis and management of various pathologies such as differentiate haemorrhage from the underlaying causative lesion, diagnosis of pulmonary embolisms, demarcation of abscess, characterization of renal stones or reduction of artifacts.

The purpose of this review is to provide the emergency radiologist a brief description of the main indications for spectral CT.

PALABRAS CLAVE
Rayos X;
Tomografía computarizada;
Emergencia;
Energía dual

TC espectral en la urgencia

Resumen La TC espectral se basa en la adquisición de imágenes de TC con rayos X a 2 niveles de energía distintos, lo que hace posible la diferenciación de los distintos materiales que presentan diferente número atómico. Esto es debido a que estos materiales presentan diferente atenuación con los distintos niveles de energía empleados, incluso aunque su atenuación sea similar a la de la TC convencional.

Este tipo de tecnología se ha generalizado debido a las importantes ventajas que ofrecen sus técnicas de posprocesado, incluyendo las imágenes sin contraste virtual, mapas de yodo, imágenes virtuales monoenergéticas o reconstrucciones mixtas, todo ello sin aumentar la dosis de radiación.

* Corresponding author.
E-mail address: hcigarran@msn.com (H. Cigarrán Sexto).

La TC espectral tiene múltiples aplicaciones en la radiología de urgencias que permiten una mejora en la detección, el diagnóstico y el manejo de distintas enfermedades.

El objetivo de esta revisión es describir brevemente las principales indicaciones de la TC espectral en urgencias.

Concept, forms of acquisition and post-processing of CT studies with spectral energy

Spectral CT technology enables greater differentiation of materials than conventional CT, based on the analysis of information from the use of X-rays with different energy levels. There are materials that have different relative absorption of X-rays emitted with different energy levels, and this makes it possible to distinguish between structures with similar density, but different elemental composition.

One subtype of spectral energy is dual-energy CT, which specifically refers to the use of two energy levels. It is the most widely used form of spectral energy in clinical practice[1].

The attenuation of materials essentially depends on photoelectric absorption and the Compton effect. Photoelectric absorption is proportional to $(Z/E)^2$, where Z is the atomic number and E is the energy of the photon. As the photon energy increases, the interaction decreases and Compton scattering, which is practically constant for different energies, becomes dominant[3]. At low voltages, the photoelectric effect predominates in elements with a high atomic number, such as calcium or iodine, which means an increase in CT attenuation.

Many different studies have shown that, overall, the radiation dose in state-of-the-art spectral equipment is similar to or even lower than conventional studies, although it does depend on the type of CT and the anatomical region studied[3–7]. Moreover, the use of virtual non-contrast (VNC) images will make it possible to reduce the dose in relation to protocols that include phases without contrast.

Spectral energy can be obtained through the use of different technologies:

- Dual-source CT, consisting of two X-ray tubes placed perpendicular to each other with different kV, usually 80 and 140 kV, but which can be independently adjusted for optimal contrast. Each tube has its own detector that works simultaneously. The advantage is essentially that there is no temporal discrepancy, and the main limitation is the small field of view of the second tube because of having to accommodate two tubes and two detectors within the gantry. A Somatom Definition Flash scanner (Siemens Healthineers) was used to conduct this study.
- CT with rapid voltage switching: a single X-ray tube is used which switches from 80 to 140 kV in less than 0.2 ms using a single detector. It has high temporal resolution with reduced spectral resolution due to the fact that the voltage cannot be modulated.
- CT with twin-beam filtration: it uses a single X-ray tube with a filter split into two parts, composed of gold and tin, which achieves spectral separation into high- and low-energy beams. It is less expensive and the filter can be placed in a conventional CT. The main disadvantages are limited spectral separation and the need for higher tube power due to filtering of the X-ray beam[8].
- CT with layer detector: it has a single tube with polychromatic spectrum and a detector with two layers of different materials. Low energies are detected in the first layer of the detector and those energies capable of passing through it are detected in the deeper layer. As spectral separation is performed at the detector level, there is perfect temporal and spatial resolution with a larger field of view than dual-source CT, but with lower spectral resolution[9,10].
- CT with sequential acquisition: two consecutive scans modifying the tube voltage. This was the first technological approach to dual energy. One limitation is that the different energy levels are not acquired at the same time, so the study takes longer and there may be changes in the arrangement of the different anatomical structures[8,11].
- Photon-counting CT: multi-energy images are obtained using a photon-counting detector, which quantifies small photon interactions to subsequently transform them into electrical energy, proportional to the magnitude of the incident ray. This electrical energy is analysed and classified into different bands based on specific energy thresholds[8].

There are various ways of post-processing the images obtained with dual energy with different clinical applications (Table 1). The types of post-processing are common to all technologies, but their names vary depending on the technology used and the manufacturer.

- Mean reconstructions: images with an appearance similar to those obtained with a CT performed at 120 kV. They are obtained by combining the source images acquired at 80 kV and at 140 kV, which can also be viewed independently.
- The maps of specific materials are obtained by detecting or estimating the basic materials (the most common are

Table 1 Spectral CT applications.

Algorithm		Clinical applications
Based on the material	Material differentiation	Differentiation of nephrolithiasis according to the atomic number
	Subtraction of materials	Differentiation between contrast and haemorrhage, since both have similar attenuation values
		Virtual non-contrast imaging: identifies and removes iodine from voxels, avoiding having to perform a non-contrast phase
		Virtual non-calcium imaging: identifies and removes calcium from bone to assess the bone marrow
		Removal of bone on CT angiography: identification and removal of bone, allowing better visualisation of the vessels with contrast
		Removal of calcified atherosclerotic plaque: better visualisation of the vessel lumen in the maximum intensity projection
	Detection of iodine	Differentiation between a solid nodule and a haemorrhagic cyst in dense kidney lesions
		Differentiation between soft and tumour thrombus
		Identification of bowel ischaemia
		Detection of active bleeding
		Differentiation of bowel content from iodine extravasation
	Fat/iron quantification	Quantitative evaluation of fatty liver disease and haemochromatosis
Based on the energy	Low-keV VMI	Enhance the presence of iodinated contrast
		Detection of cholesterol gallstones
	High keV VMI	Reduction of metal artefacts
		Detection of pulmonary thromboembolism
	Z_{eff} maps	Demonstration of inflammatory activity
		Detection of cholesterol gallstones

VMI: virtual monoenergetic images; Z_{eff}: effective atomic number.

water and iodine) to later make a representation of their distribution.

- The subtracted iodine/water can be presented as pure maps or superimposed on grey-scale images, enabling a qualitative and quantitative analysis of the presence of these substances.
- Decomposition of the value of any voxel in the contribution of each of its components allows materials to be subtracted. Removal of iodine produces VNC images similar to CT without contrast administration. Calcium removal provides virtual non-calcium images (VNCa).
- Virtual monoenergetic images (VMI) allow the HU of each tissue to be simulated at a single energy level, which can range from 40 to 200 keV. The use of images with low kilovoltage highlights structures that contain iodine, while in those with high kilovoltage the presence of iodine is attenuated and metal artefacts are reduced[12,13].
- Z effective (Z_{eff}) number maps make it possible to obtain colour images based on the atomic number of the materials. In enhanced masses it aids the diagnosis, and in kidney stones a low atomic number helps guide uric acid calculation[14,15].
- X-map: this is a virtual map of grey matter that can differentiate between cerebral parenchyma and water, facilitating the detection of cerebral oedema[16,17].
- Other widely-used reconstructions, such as fat fraction mapping or quantitative iron mapping, have fewer applications in medical emergencies.

Applications of spectral CT in emergency radiology

General applications

Potentiation of the effect of iodinated contrast

Spectral energy makes it possible to increase vascular enhancement by increasing iodine attenuation in low-keV VMI reconstructions. This means that a smaller volume of contrast can be used, and we can assess small-lumen vessels and improve the diagnostic quality of poorly opacified studies[18].

Reduction of artefacts

Metals produce partial or complete attenuation of low-energy X-rays, causing hardening artefacts. VMI with high keV avoid contamination deriving from attenuated rays that do not reach the detector, thereby causing artefacts, but entail a loss of contrast resolution between the different tissues[19].

Head and neck

Detection of lesions

VMI help to detect low-density images or haemorrhages on non-contrast CT, although the energy level depends on the location of the lesion. Lesions which are hypodense in white

matter or hyperdense in grey matter are best detected at low keV[20].

Furthermore, X maps increase the sensitivity to detect oedema induced by acute cerebral ischaemia, allowing early detection of ischaemic changes and aiding selection of patients who are candidates for mechanical thrombectomy[16].

Post-traumatic haemorrhage

An increase in density on CT can be caused by calcium or blood. The use of VNCa maps helps increase diagnostic certainty. Bone subtraction techniques enable small subdural haemorrhages or peripheral contusions to be identified by removing adjacent dense bone[21].

Spontaneous bleeding

Spontaneous intraparenchymal haemorrhages may be secondary to underlying lesions (vascular, neoplastic or infectious).

The use of intravenous (IV) contrast-enhanced spectral CT enables identification of any underlying lesion within an intraparenchymal haematoma by detecting areas of iodine uptake (Fig. 1A)[19,22].

Post-thrombectomy

In follow-up after mechanical thrombectomy, a common finding is increased attenuation in the ischaemic territory, which may be secondary to extravasation of contrast due to disruption of the blood-brain barrier or haemorrhagic transformation.

Dual energy makes it possible to determine the origin of the hyperdensity with high sensitivity and specificity. If the origin is haemorrhagic, only hyperdensity persists on VNC maps, while contrast retention only remains visible on iodine maps[23]. The overall analysis of both maps will make it possible to quantify each component in the event that there is a mixture of the two (Fig. 1B and C).

Venous thrombosis

As it is not enhanced by contrast, the thrombus is not represented on the iodine map, but low-keV VMI increase the difference in density between the thrombus and the opacified sinus, increasing sensitivity[24].

Cervical spine abscesses

Spectral energy enables more accurate delineation of the extent of the collection and adjacent inflammation by using Z_{eff} maps and low-keV VMI. In addition, demonstration of proximity to vascular structures may be beneficial to prevent bleeding in case of the need for surgical drainage[19].

Chest

Pulmonary thromboembolism

The use of Z_{eff} and iodine maps increases the sensitivity for the detection of pulmonary thromboembolism, as it allows the simultaneous study of arterial filling defects, which would be shown in a different colour, and areas of hypoperfusion, visible as triangular-shaped iodine uptake defects in the parenchyma. This is particularly relevant in the diagnosis of small peripheral emboli which, without treatment, could evolve into pulmonary hypertension[25].

In cases of non-occlusive pulmonary embolism, iodine maps can demonstrate normal lung perfusion distal to partial filling defects (Fig. 2).

Abdomen

Detection of active bleeding

This principle is applicable to any anatomical region. Spectral energy makes it possible to dispense with the non-contrast phase, as VNC reconstructions are available, and so reduces radiation dose and acquisition time. Iodine maps and VMI at low keV help to detect small volumes of extravasated contrast, increasing the sensitivity for the detection of active bleeding, with greater precision when determining the origin, which can be masked by the presence of adjacent dense clots (Fig. 3A)[26].

Assessment of contrast enhancement

Differentiating clots from an underlying neoplastic lesion. As in spontaneous cerebral haemorrhages, in other anatomical regions the presence of blood makes it difficult to detect underlying contrast-enhancing lesions, as both are hyperdense and have similar attenuation values. Analysis of the iodine maps and VMI at low keV makes it possible to differentiate between each component (Fig. 3B). Wunderlich syndrome or frank haematuria secondary to a bladder tumour are examples of its utility[19].

Venous thrombosis

Iodine maps and quantification, as well as the assessment of the VMI at low keV, make it possible to detect the presence of contrast in tumour thrombi, a fundamental criterion for their differentiation from soft thrombi[27]. In patients with hepatocellular carcinoma, an iodine quantification greater than 0.9 mg/mL differentiates between the two lesions with high sensitivity and specificity[28].

Bowel ischaemia

Bowel ischaemia is caused by decreased or absent blood flow in a loop[26]. The most specific sign is the absence of or decrease in enhancement of the bowel wall, which may go unnoticed in the initial phases of a conventional CT. Both iodine maps and low-keV VMI facilitate early detection of low mural uptake, either by visual qualitative analysis or by absolute (calculation of the iodine density in the hypoperfused loop) and relative (comparing the iodine densities of the hypoperfused loop and the normal loop) quantitative analysis, more suitable because it is not influenced by haemodynamic factors (Fig. 4A)[29].

In this context, the presence of mural hyperdensity may mean haemorrhage or hypervascularisation due to reperfusion. The distinction can be made by analysing the VNC images[30].

Inflammatory bowel disease

Analysis of a spectral CT performed in the portal phase with low-keV VMI makes it possible to increase the differences in attenuation between inflamed and normal loops, while

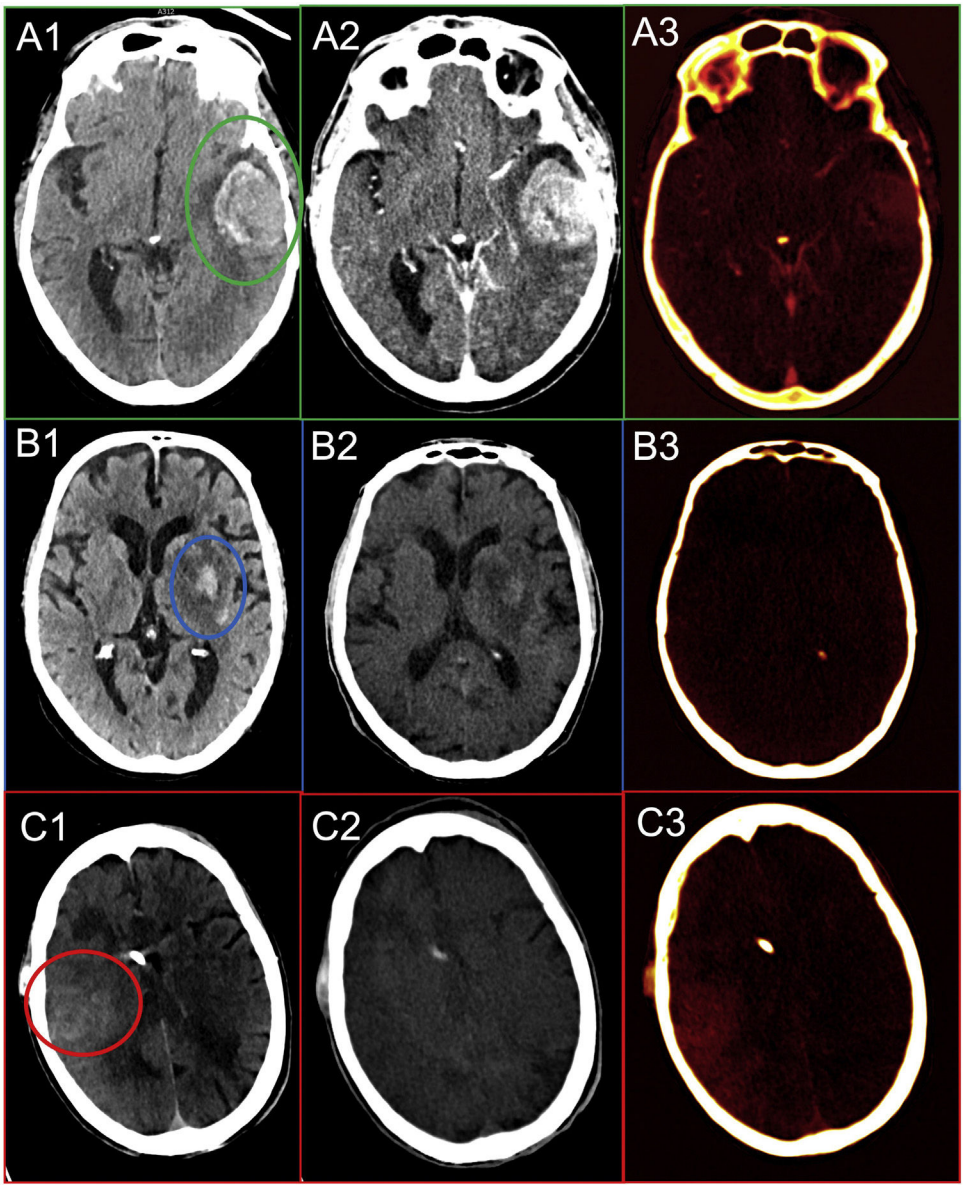

Figure 1 A) Secondary haemorrhage. Non-contrast CT with left temporal haematoma (green circle) (1). Mean CT with IV contrast showing a slight increase in density (2). Iodine map confirming an underlying neoplastic lesion as the source of bleeding (3). B) Haemorrhagic transformation. Mean CT in a patient undergoing mechanical thrombectomy with subacute ischaemic lesion in the left basal ganglia with two hyperdense areas in the lentiform nucleus (blue circle) (1). The virtual non-contrast map shows hyperdensity in the lentiform nucleus, so it can be ruled out that it is contrast, in fact corresponding to bleeding foci (2). The iodine map does not show contrast enhancements (3). C) Contrast retention. Mean CT with right temporal/parietal hyperdensity (red circle) (1). Virtual non-contrast CT does not show hyperdensities (2). The iodine map shows a temporal/parietal uptake representing contrast retention (3).

the iodine and Z_{eff} maps quantify the difference in iodine uptake, relevant when establishing disease activity[19].

Pancreatic disease

CT is the modality of choice in patients with pancreatitis who require an imaging technique for assessment. The use of iodine maps increases sensitivity for detecting glandular inflammation, as the iodine density significantly decreases (less than 2.1 mg/mL) compared to the normal pancreas, while non-perfused necrotic areas can also be distinguished. Low-keV VMI provide better definition of complex collections and make it easier to detect vascular complications such as thrombosis or pseudoaneurysms (Fig. 4B)[31].

As in other organs such as the liver or spleen, low-keV VMI make it easier to detect small lacerations, which are difficult to identify in the pancreas because acquisition is usually in the venous phase and not in the late arterial phase[31,32].

Small pancreatic tumours can also be difficult to distinguish on conventional CT. Low-keV VMI, Z_{eff} or iodine maps allow a better definition of pancreatic hypo- or hypervascular lesions, facilitating the detection and diagnosis of cancer.

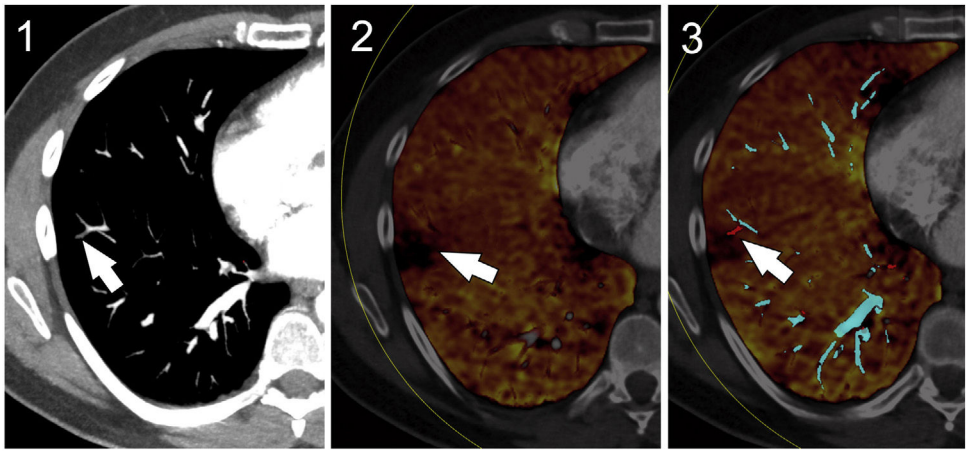

Figure 2 Pulmonary thromboembolism. CT angiogram of the pulmonary arteries with suspected filling defect in the subsegmental artery (white arrow) (1). Iodine map showing a peripheral perfusion defect consistent with the thrombus (white arrow) (2). Iodine map associated with effective atomic number (Zeff) map showing the different composition of the thrombosed artery (white arrow) (3).

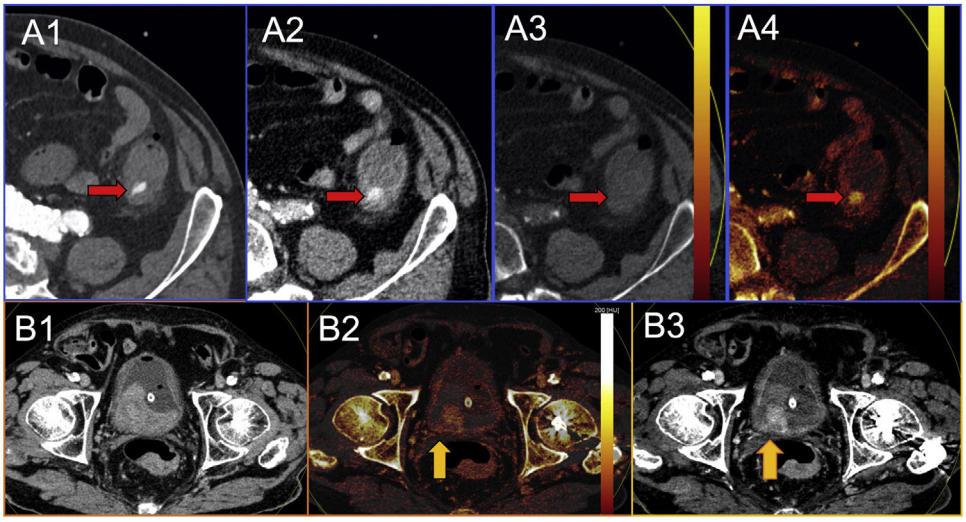

Figure 3 A) Active bleeding. Abdominal CT in the arterial phase showing hyperdensity in the descending colon (red arrow), which could correspond to active bleeding (1). In the mean portal phase there is no evident increase in contrast extravasation (red arrow), which makes the diagnosis of active bleeding suspect (2). The virtual non-contrast reconstruction shows disappearance of the hyperdensity (red arrow) (3). The iodine map shows that the hyperdensity corresponds to extravasated contrast. The findings of the virtual non-contrast map and the iodine map mean the diagnosis of active bleeding can be made with certainty (4). B) Neoplastic lesion with an adjacent clot. Abdominal CT in mean portal phase. Extensive occupation of the bladder by a high-density material (1). Iodine map shows a solid contrast-enhancing lesion (yellow arrow) attached to the right posterior wall of the bladder in association with a neoplasia. The other dense areas correspond to a voluminous clot (2). Low-keV VMI, where we enhanced the contrast uptake areas of the neoplasia (yellow arrow) (3).

Cholecystitis

Although ultrasound is the most sensitive technique in the assessment of gallbladder disease, CT is also common in certain cases. Portal phase spectral CT enables quantitative analysis of gallbladder wall enhancement with high sensitivity. Low-energy VMI and iodine maps are useful for detecting wall hyperenhancement in acute cholecystitis or low uptake and focal areas of non-enhancement associated with necrosis in gangrenous cholecystitis (Fig. 5)[33].

Pyelonephritis and renal infarction

Pyelonephritis and renal infarction can have a similar clinical presentation, and both are identified as hypodense images on portal-phase CT. The VMI show better delimitation of the lesions, while the iodine and Z_{eff} maps quantify the presence of iodine, which is decreased in pyelonephritis and absent in renal infarction[19].

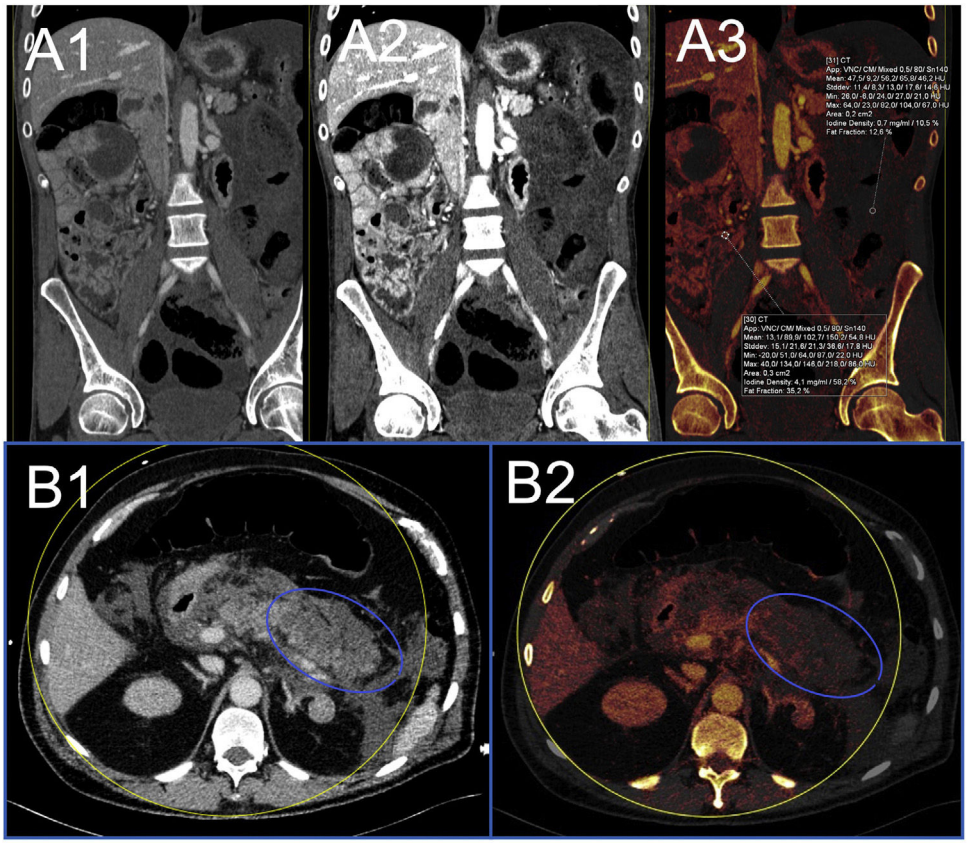

Figure 4 A) Bowel ischaemia. Abdomen CT in mean portal phase in the coronal plane showing marked low uptake of the bowel loops on the left flank with free fluid (1). The same image with virtual monoenergetic reconstructions at low keV where the low uptake is more evident (2). The iodine map shows a much lower iodine density in loops with low uptake (0.7 mg/mL) than in non-diseased loops (4.1 mg/mL) (3). B) Acute pancreatitis. Oedema of the pancreas and extensive peripancreatic inflammatory changes (1). The iodine map identifies an area of poor enhancement in the tail of pancreas (blue circle), findings consistent with necrosis in the context of acute necrotising pancreatitis (2).

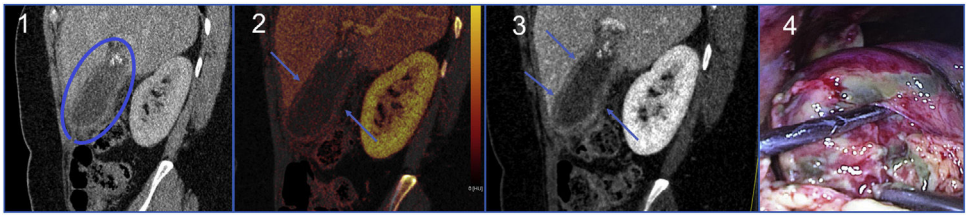

Figure 5 Gangrenous cholecystitis. Abdomen CT in portal phase showing diffuse thickening of the gallbladder wall with cholelithiasis and peri-vesicular oedema (blue circle) in association with acute cholecystitis (1). Iodine map showing areas of decreased uptake of the gallbladder wall (blue arrows) secondary to necrosis associated with gangrenous cholecystitis (2). Low-keV VMI where patchy areas are best identified without contrast (blue arrows) (3). Surgical specimen where necrotic patchy areas can be seen (4).

Detection and characterisation of lithiasis

Nephrolithiasis. CT is the most sensitive test for detecting kidney stones, their size and location, as well as complications such as dilation of the excretory tract and renal or peri-renal oedema.

Spectral CT makes it possible to characterise calculi based on their composition with a sensitivity of 90–100 %. Uric acid stones attenuate high-energy radiation more due to the presence of elements with low atomic number, while calcium oxalate or calcium phosphate stones attenuate lower-energy radiation more because they are made up of elements with higher atomic number. VNC reconstructions facilitate the detection of nephrolithiasis in abdominal studies performed with IV contrast, and ureteral or bladder lithiasis when the excretory tract is opacified with contrast[19].

Cholelithiasis and choledocholithiasis

Detection of gallstones on CT depends on the composition and size of the stone. Cholesterol gallstones have a density similar to bile and are not detectable on conventional CT, but they can be detected using spectral energy.

Table 2 Limitations of spectral CT.

When does it happen?	What causes it?	What happens?	Possible solution
During the acquisition	High body mass index	Noise Inadequate decomposition of materials Photon starvation artefact	Maximum weight limit: 118—127 kg Transverse diameter limit: 38—46 cm Change in acquisition variables. In dual-source CT: increase the low-kilovoltage beam from 80 to 100 kVp
	Patient position in the gantry	Lack of spectral information as outside the field of view	In dual-source CT the maximum field of view is 26—35.5 cm. Proper placement in the gantry according to the anatomical area to be studied
	Placement of the arms	Beam-hardening artefact	Arms placed above or below the shoulders according to the region to be studied: head-neck/chest-abdomen
	Contrast medium density	Significant increase in contrast density in low-kilovoltage images *Blooming* Inadequate iodine suppression on virtual non-contrast images	Reducing the concentration of the oral or intravenous contrast administered
	Inadequate temporal resolution	Spectral bias: on CT based on the X-ray source, there is a time lag for obtaining each voxel with dual energy	Increase tube rotation speed
During the post-processing	Low-energy photon counting	Hyperdense foci on iodine maps False urate deposits	Adequate reconstruction filter Appropriate selection of attenuation threshold
	Inadequate selection of threshold	False positives/negatives Inadequate separation of materials Increased noise	Adequate selection of the material decomposition threshold taking into account the disease to be studied and tube voltage Adjustment of the voltage pairs predefined by the manufacturer based on clinical experience: 80/140 or 100/140 kVp
During the visualisation	Inadequate window	*Blooming in low-kilovoltage images* False enhancement Visualisation of iodine in subcutaneous fat or air	Window level and width should be adjusted using fat, air and fluid as a model

The attenuation curve of fat is inverse to that of iodine, so cholesterol gallstones are hypoattenuating in low-keV VMI and hyperattenuating in high keV VMI. Calcified stones are best detected on VNC reconstructions.

Z_{eff} maps enable differentiation of the calculus from the surrounding fluid in the case of gallstone ileus[19,26].

Incidental lesions

Spectral energy makes it possible to characterise incidental lesions, which very often cannot be characterised in a single-phase scan.

This is common with adrenal nodules. VNC reconstructions allow their density to be determined; as this may be slightly higher than in true non-contrast scans, there is a risk of classifying more lesions as indeterminate. However, the diagnosis of adenoma can be made with certainty using a threshold below 10 HU[34]. The finding of dense renal cysts is also common; absence of uptake can be demonstrated on the iodine maps.

This avoids the need to repeat tests, with the consequent reduction in healthcare costs and radiation dose.

Musculoskeletal system

Acute fractures

The oedema or haemorrhage in the bone marrow that accompanies acute fractures is not identifiable on conventional CT because the cancellous bone obscures visualisation of the marrow. With spectral CT we can perform VNCa, which subtracts the cancellous bone, so we can then analyse the bone marrow density and attenuation will be higher if there is oedema or haemorrhage. This application makes

it possible to diagnose subtle fractures or date the age of a vertebral compression fracture[19,26].

Uric acid deposits

The same principle that enables the composition of nephrolithiasis to be characterised in abdominal scans can be applied to other fields, such as the detection of uric acid deposits in musculoskeletal studies, making it possible to diagnose gouty arthritis[19].

Limitations

As well as the limitations inherent in each type of acquisition technology, spectral CT generates a larger number of images, which then require more interpretation time and greater storage capacity in PACS.

Conducting studies with dual energy does not increase room occupation time, but the systematic review of the different reconstructions increases the workload for the radiologist.

In addition, dual energy produces a series of artefacts (Table 2) that have to be recognised and corrected by the radiologist to avoid diagnostic errors.

Practical recommendations

As it is still a relatively recent and expensive technology, the availability of this equipment tends to be limited, hence not all urgent studies can be performed using spectral CT.

At our hospital, at present, we use dual-energy CT for all scans that would require a non-contrast phase (mesenteric ischaemia, suspected active bleeding and gastrointestinal bleeding), those where we need assessment of organ perfusion (pulmonary thromboembolism, pancreatitis, suspected gangrenous cholecystitis on ultrasound), contrast studies in spontaneous cerebral haemorrhages, follow-up after mechanical thrombectomy, for nephrolithiasis not visualised on ultrasound needing characterisation, and for peripheral vascular studies. The study of these patients always includes a review of the VNC reconstructions, VMI and iodine maps. The use of other reconstructions is less common (Z_{eff} maps, VNCa), reserved only for specific cases and depending on the disease studied.

We automatically send the high- and low-kV source images to the PACS, as well as the mean reconstructions that would allow the study to be visualised without the need for post-processing. Recovery of the source images from the specific workstations means we can defer any post-processing. The rest of the post-processed images, as well as the most representative images of the disease findings identified, are sent to the PACS at the discretion of the radiologist[34].

Conclusion

Although the concept of spectral power is not recent, technological advances and greater availability have made it possible to expand its use in emergency scans. There are now multiple applications of spectral CT in the detection, diagnosis and management of different acute diseases, a list of indications that continues to grow with the consequent improvement in diagnostics.

Acronyms

VMI: virtual monoenergetic images.
VNC: virtual non-contrast.
VNCa: virtual non-calcium.
Z_{eff} maps: effective atomic number maps.
PACS: Picture Archiving and Communication System.

Ethical considerations

The consent of the Ethics Committee was not necessary because the studies were conducted for clinical indication and not for research purposes. Consent was obtained from the patients to perform the imaging studies. None of the images shows data that could identify the patients.

Authorship

1 Responsible for the integrity of the study: HCS, JCB and GFS.
2 Study conception: HCS, JCB and GFS.
3 Study design: HCS, JCB and GFS.
4 Data collection: HCS, JCB and GFS.
5 Data analysis and interpretation: HCS, JCB and GFS.
6 Statistical processing: HCS, JCB and GFS.
7 Literature search: HCS, JCB and GFS.
8 Drafting of the article: HCS, JCB and GFS.
9 Critical review of the manuscript with intellectually relevant contributions: HCS, JCB and GFS.
10 Approval of the final version: HCS, JCB and GFS.

Conflicts of interest

The authors declare that they have no conflicts of interest.

References

1. So A, Nicolaou S. Spectral computed tomography: Fundamental principles and recent developments. Korean J Radiol. 2021;22:86–96, http://dx.doi.org/10.3348/kjr.2020.0144. Epub 2020 Sep 10.
2. Henzler T, Fink C, Schoenberg SO, Schoepf UJ. Dual-energy CT: Radiation dose aspects. AJR Am J Roentgenol. 2012;199:S16–25, http://dx.doi.org/10.2214/AJR.12.9210. Erratum en: AJR Am J Roentgenol. 2013;200:705.
3. Parry RA, Glaze SA, Archer BR. The AAPM/RSNA physics tutorial for residents. Typical patient radiation doses in diagnostic radiology. Radiographics. 1999;19:1289–302, http://dx.doi.org/10.1148/radiographics.19.5.g99se211289.
4. Tawfik AM, Kerl JM, Razek AA, Bauer RW, Nour-Eldin NE, Vogl TJ. Image quality and radiation dose of dual-energy CT of the head and neck compared with a standard 120-kVp acquisition. AJNR Am J Neuroradiol. 2011;32:1994–9, http://dx.doi.org/10.3174/ajnr.A2654. Epub 2011 Sep 8.
5. Forghani R, de Man B, Gupta R. Dual-energy computed tomography: Physical principles, approaches to scanning, usage, and implementation: Part 1. Neuroimaging Clin N Am. 2017;27:371–84, http://dx.doi.org/10.1016/j.nic.2017.03.002.

6. Forghani R, de Man B, Gupta R. Dual-energy computed tomography: Physical principles, approaches to scanning, usage, and implementation: Part 2. Neuroimaging Clin N Am. 2017;27:385–400, http://dx.doi.org/10.1016/j.nic.2017.03.003.
7. Van Ommen F, de Jong HWAM, Dankbaar JW, Bennink E, Leiner T, Schilham AMR. Dose of CT protocols acquired in clinical routine using a dual-layer detector CT scanner: A preliminary re-port. Eur J Radiol. 2019;112:65–71, http://dx.doi.org/10.1016/j.ejrad.2019.01.011. Epub 2019 Jan 14.
8. Alavandar E, Arunachalam VK, Narappulan N, Mahadevan GS, Kashyap R, Mehta P, et al. Principles and available hardware in DECT. Journal Gastrointestinal and Abdominal Radiology. 2022;01:1–74, http://dx.doi.org/10.1055/s-0042-1742772.
9. Forghani R, de Man B, Gupta R. Dual-energy computed tomography: Physical principles, approaches to scanning, usage, and implementation: Part 1. Neuroimaging Clin N Am. 2017;27:371–84, http://dx.doi.org/10.1016/j.nic.2017.03.002.
10. Johnson TR. Dual-energy CT: General principles. AJR Am J Roentgenol. 2012;199:S3–8, http://dx.doi.org/10.2214/AJR.12.9116.
11. Aran S, Shaqdan KW, Abujudeh HH. Dual-energy computed tomography (DECT) in emergency radiology: Basic principles, techniques, and limitations. Emerg Radiol. 2014;21:391–405, http://dx.doi.org/10.1007/s10140-014-1208-2. Epub 2014 Mar 28.
12. McCollough CH, Boedeker K, Cody D, Duan X, Flohr T, Halliburton SS, et al. Principles and applications of multienergy CT: Report of AAPM Task Group 291. Med Phys. 2020;47:e881–912, http://dx.doi.org/10.1002/mp.14157. Epub 2020 May 28. Erratum en: Med Phys. 2021;48:2694.
13. Agostini A, Borgheresi A, Mari A, Floridi C, Bruno F, Carotti M, et al. Dual-energy CT: Theoretical principles and clinical applications. Radiol Med. 2019;124:1281–95, http://dx.doi.org/10.1007/s11547-019-01107-8. Epub 2019 Dec 2.
14. Rajiah P, Parakh A, Kay F, Baruah D, Kambadakone AR, Leng S. Update on multienergy CT: Physics, principles, and applications. Radiographics. 2020;40:1284–308, http://dx.doi.org/10.1148/rg.2020200038. Epub 2020 Aug 21.
15. Adam SZ, Rabinowich A, Kessner R, Blachar A. Spectral CT of the abdomen: Where are we now? Insights Imaging. 2021;12:138, http://dx.doi.org/10.1186/s13244-021-01082-7.
16. Mohammed MF, Marais O, Min A, Ferguson D, Jalal S, Khosa F, et al. Unenhanced dual-energy computed tomography: Visualization of brain edema. Invest Radiol. 2018;53:63–9, http://dx.doi.org/10.1097/RLI.0000000000000413. PMID: 28915161.
17. Kaichi Y, Tatsugami F, Nakamura Y, Baba Y, Iida M, Higaki T, et al. Improved differentiation between high- and low-grade gliomas by combining dual-energy CT analysis and perfusion CT. Medicine (Baltimore). 2018;97:e11670.
18. Aran S, Daftari Besheli L, Karcaaltincaba M, Gupta R, Flores EJ, Abujudeh HH. Applications of dual-energy CT in emergency radiology. AJR Am J Roentgenol. 2014;202:W314–24, http://dx.doi.org/10.2214/AJR.13.11682. Erratum en: AJR Am J Roentgenol. 2014;202:1396. Besheli, Laleh Daftari [corrected to Daftari Besheli, Laleh].
19. Demirler Simsir B, Danse E, Coche E. Benefit of dual-layer spectral CT in emergency imaging of different organ systems. Clin Radiol. 2020;75:886–902, http://dx.doi.org/10.1016/j.crad.2020.06.012. Epub 2020 Jul 18.
20. Lennartz S, Laukamp KR, Neuhaus V, Große Hokamp N, Le Blanc M, Maus V, et al. Dual-layer detector CT of the head: Initial experience in visualization of intracranial hemorrhage and hypodense brain lesions using virtual monoenerget-ic images. Eur J Radiol. 2018;108:177–83, http://dx.doi.org/10.1016/j.ejrad.2018.09.010. Epub 2018 Sep 11.
21. Naruto N, Tannai H, Nishikawa K, Yamagishi K, Hashimoto M, Kawabe H, et al. Dual-energy bone removal computed tomography (BRCT): Preliminary report of efficacy of acute intracranial hemorrhage detection. Emerg Radiol. 2018;25:29–33, http://dx.doi.org/10.1007/s10140-017-1558-7. Epub 2017 Sep 20.
22. Kim SJ, Lim HK, Lee HY, Choi CG, Lee DH, Suh DC, et al. Dual-energy CT in the evaluation of intracerebral hemorrhage of unknown origin: Differentiation between tumor bleeding and pure hemorrhage. AJNR Am J Neuroradiol. 2012;33:865–72, http://dx.doi.org/10.3174/ajnr.A2890. Epub 2012 Jan 12.
23. Tijssen MP, Hofman PA, Stadler AA, van Zwam W, de Graaf R, van Oostenbrugge RJ, et al. The role of dual energy CT in differentiating between brain haemor-rhage and contrast medium after mechanical revascularisation in acute ischaemic stroke. Eur Radiol. 2014;24:834–40, http://dx.doi.org/10.1007/s00330-013-3073-x. Epub 2013 Nov 21.
24. Weiss J, Schabel C, Othman AE, Bier G, Nikolaou K, Bamberg F, et al. Impact of dual-energy CT post-processing to differentiate venous thrombosis from iodine flux artefacts. Eur Radiol. 2018;28:5076–82, http://dx.doi.org/10.1007/s00330-018-5534-8. Epub 2018 Jun 4.
25. Otrakji A, Digumarthy SR, lo Gullo R, Flores EJ, Shepard JA, Kalra MK. Dual-energy CT: Spec-trum of thoracic abnormalities. Radiographics. 2016;36:38–52, http://dx.doi.org/10.1148/rg.2016150081.
26. Wortman JR, Uyeda JW, Fulwadhva UP, Sodickson AD. Dual-energy CT for abdominal and pelvic trauma. Radiographics. 2018;38:586–602, http://dx.doi.org/10.1148/rg.2018170058.
27. Agrawal MD, Pinho DF, Kulkarni NM, Hahn PF, Guimaraes AR, Sahani DV. Oncologic applications of dual-energy CT in the abdomen. Radiographics. 2014;34:589–612, http://dx.doi.org/10.1148/rg.343135041.
28. Ascenti G, Sofia C, Mazziotti S, Silipigni S, d'Angelo T, Pergolizzi S, et al. Dual-energy CT with iodine quantification in distinguishing between bland and neoplastic portal vein thrombosis in patients with hepatocellular carcinoma. Clin Radiol. 2016;71:938.e1–9, http://dx.doi.org/10.1016/j.crad.2016.05.002. Epub 2016 May 27.
29. Lourenco PDM, Rawski R, Mohammed MF, Khosa F, Nicolaou S, McLaughlin P. Dual-energy CT Iodine Mapping and 40-keV monoenergetic applications in the diagnosis of acute bowel ischemia. AJR Am J Roentgenol. 2018;211:564–70, http://dx.doi.org/10.2214/AJR.18.19554. Epub 2018 Jun 21.
30. Cigarrán Sexto H, Clavo Blanco J. Isquemia visceral y mesentérica. In: Marti M, Vicente A, editors. Tratado de Radiología de Urgencias. Madrid: Editorial Médica Panamericana; 2022. p. 359–72.
31. Mastrodicasa D, delli Pizzi A, Patel BN. Dual-energy CT of the pancreas. Semin Ultrasound CT MR. 2019;40:509–14, http://dx.doi.org/10.1053/j.sult.2019.05.002. Epub 2019 Jun 11.
32. Wichmann JL, Majenka P, Beeres M, Kromen W, Schulz B, Wesarg S, et al. Single-portal-phase low-tube-voltage dual-energy CT for short-term follow-up of acute pancreatitis: Evaluation of CT severity index, interobserver agreement and radiation dose. Eur Radiol. 2014;24:2927–35,

http://dx.doi.org/10.1007/s00330-014-3300-0. Epub 2014 Jul 17. PMID: 25030462.
33. Singh T, Gupta P. Role of dual energy computed tomography in gallbladder disease: A review. J Gastrointestinal Abdominal Radiol ISGAR. 2022;05:107–13, http://dx.doi.org/10.1055/s-0042-1743173.
34. Parakh A, An C, Lennartz S, Rajiah P, Yeh BM, Simeone FJ, et al. Recognizing and minimizing artifacts at dual energy. Radiographics. 2021;41:509–23, http://dx.doi.org/10.1148/rg.20212000049.